Available online at www.sciencedirect.com

SciVerse ScienceDirect

Ceramics International 39 (2013) 3221–3229

CERAMICS INTERNATIONAL

www.elsevier.com/locate/ceramint

Recovery of mechanical strength by surface crack disappearance via thermal oxidation for nano-Ni/Al_2O_3 hybrid materials

Daisuke Maruoka[a], Makoto Nanko[b,*]

[a]Graduate School of Engineering, Nagaoka University of Technology, Nagaoka 940-2188, Japan
[b]Department of Mechanical Engineering, Nagaoka University of Technology, Nagaoka 940-2188, Japan

Received 5 March 2012; received in revised form 4 September 2012; accepted 1 October 2012
Available online 11 October 2012

Abstract

Recovery of mechanical strength as a function of heat-treatment temperature and time was investigated in α-Al_2O_3-based hybrid materials containing with 5 vol% dispersed Ni nanoparticles (nano-Ni/Al_2O_3) via fraction of surface crack disappearance. Surface cracks introduced by Vickers indentation disappeared completely because of the oxidation product $NiAl_2O_4$. Bending strengths of as-sintered and as-cracked samples were 490 ± 58 and 180 ± 15 MPa, respectively. Heat-treatment at 1000 °C for 1 h resulted in recovery of bending strength up to 550 ± 190 MPa with 10% fraction of crack disappearance. The bending strength of samples heat-treated at higher temperatures or for longer durations was comparable with that of the as-sintered samples. Bending strength reached and remained at approximately 604 MPa when the fraction of surface crack disappearance was over 55%. As-recovered samples did not fracture at the surface cracks during the three-point bending test. Thus, recovery of mechanical strength was achieved by partial disappearance of the surface cracks.

This observed recovery of mechanical strength was caused by a reduction in stress concentration at crack-tips covered with $NiAl_2O_4$ formed from Ni^{2-} along grain boundaries of the Al_2O_3 matrix.

Keywords: Nanocomposites; Al_2O_3; Self-healing; Corrosion

1. Introduction

Alumina ceramics have high mechanical strength and chemical stability, excellent high-temperature resistance and low production cost among structural engineering ceramics. They have been widely applied as cutting tools and high-temperature gas filters. However, their ductility and fracture toughness are insufficient for structural materials owing to a high susceptibility to surface cracking [1]. These disadvantages cause the mechanical strength to be sensitive to surface cracks. Surface finishing for removing surface cracks such as polishing is consequently required, resulting in high production cost for these ceramic materials. In addition, sensitivity to surface cracks reduces the mechanical reliability of alumina ceramics. Thus, the potential of alumina ceramics cannot be utilized to compensate for the lowest mechanical strength. Surface cracks may form during high-temperature operation, leading to catastrophic fracture. Management of surface cracks of importance increase the potential applications of alumina ceramics.

Crack-healing function in ceramic-based composites was discovered by Ando and his co-workers [2]. Non-oxide dispersoids in such ceramics are oxidized within surface cracks by heat-treatment, and the resulting oxidation product fills the cracks. As a result, the mechanical strength is recovered up to the level of polished samples. This crack-healing function extends the life time of ceramic components and results in easy maintenance. SiC dispersoid is typically used for crack-healing function in ceramic-based composites [2–13]. Takahashi et al. [10] reported the crack-healing function of 20 vol% SiC whiskers dispersed in Al_2O_3 matrix. The samples were heat-treated at temperature ranging from 1000 to 1300 °C for 1 h in air after

*Correspondence to: Department of Mechanical Engineering, Nagaoka University of Technology, 1603-1, Kamitomioka, Nagaoka, Niigata, 940-2188, Japan. Tel./fax: +81 258 47 9768.
E-mail address: nanko@mech.nagaokaut.ac.jp (M. Nanko).

0272-8842/$ - see front matter © 2012 Elsevier Ltd and Techna Group S.r.l. All rights reserved.
http://dx.doi.org/10.1016/j.ceramint.2012.10.008

introducing pre-cracks approximately 100 μm in length by Vickers indentation. The obtained three-point bending strength of the composite was approximately 1000 MPa after heat-treatment, while the bending strength of the as-cracked sample was as only as 440 MPa. However, bending strength of crack-healed specimens increased with heat-treatment temperature and reached 970 and 980 MPa similar to that of as-polished specimens, after heat-treatment at 1200 and 1300 °C for 1 h in air, respectively. Osada et al. [11] reported the crack-healing effectiveness of 15 vol% dispersed SiC particles in Al_2O_3 matrix after machining. Samples prepared for bending tests were machined to create semicircular groove at the center of each smooth sample and heat-treated at 1300 to 1400 °C for 1 and 10 h in air. As a result, while the bending strength of as-machined samples ranged from 200 to 400 MPa, bending strength was increased after heat-treatment to up to 845 MPa comparable with that of as-received samples. The healed cracks indicated that they had been filled with SiO_2.

Crack-healing function has also been investigated for NiAl in Al_2O_3 matrix [14]. With respect to Al_2O_3 matrix containing TiC or ZrO_2 dispersoids, mechanical strength was not recovered completely by thermal oxidation [15].

The author's group has previously reported the surface crack disappearance in hybrid materials comprising 5 vol% Ni nanoparticles dispersed in Al_2O_3 matrix (nano-Ni/Al_2O_3) [16,17]. Nano-Ni/Al_2O_3 is known as a nanocomposite materials [18] that reinforces ceramics material to give improved mechanical strength and fracture toughness [19–23]. Because nano-Ni/Al_2O_3 contains metallic Ni nanoparticles, it is expected to have additional useful properties such as magnetism [24]. Surface cracks introduced by Vickers indentation were filled with the oxidation product, $NiAl_2O_4$, and mechanical recovery took place. Bending strengths of as-cracked samples attained comparable values to those of as-sintered ones when pre-cracks completely disappeared by heat-treatment at 1200 °C for 6 h in air.

Although a crack-healing function was discovered in nano-Ni/Al_2O_3, how the crack-healing function is influenced by heat-treatment conditions such as temperature, time, atmosphere and defect size have not been well-investigated. To extend the industrial applications of such crack-healing alumina composites, thermal oxidation at lower temperature and for shorter duration is very important. In this study, recovery of mechanical strength in nano-Ni/Al_2O_3 was investigated at various heat-treatment temperatures and times. Furthermore, the relationship between recovery of mechanical strength and fraction of surface crack disappearance is very important. Complete surface crack disappearance may be unnecessary for complete recovery of mechanical strength. Partial disappearance of surface cracks until they reach the intrinsic defect size was expected to result in the mechanical strength to as-sintered samples.

2. Experimental procedures

Specimens used in this study were 5 vol% nano-Ni/Al_2O_3 produced by a pulsed electric current sintering (PECS) technique. The starting powder mixture was prepared by drying, a distilled water slurry of α-Al_2O_3 (Sumitomo Chemical Co. Ltd, AA-04, average particle size: 0.44 μm, purity 99.99%) and Ni $(NO_3)_2 \cdot 6H_2O$ (Kojundo Chemical Laboratory Co. Ltd, purity 99.9%). After drying at 400 °C and then milling the powder mixture with a alumina mortar for 10 min, it was reduced at 600 °C for 12 h in a stream of Ar-1% H_2 gas mixture. The reduced powder mixture was identified by X-ray diffraction (XRD) as being composed of only Ni and α-Al_2O_3. The powder mixture was densified in a graphite die by PECS at a die temperature of 1400 °C under 40 MPa uni-axial pressure in a vacuum for 5 min holding time. Fabricated sintered samples with relative density of at least 99% of the theoretical value were used in the present study. Fig. 1 shows a scanning electron microscope (SEM) image of the fractured surface of an as-sintered sample. Ni particles, observed as bright contrast dots, were homogeneously dispersed in the sample. The average particle size of these Ni particles was approximately 300 nm, while the average Al_2O_3 grain size was approximately 1.1 μm.

As-sintered samples were cut into a rectangular shape (3 × 4 × 26 mm) for bending tests. The sample surface was ground using a grinding wheel with 30 μm-diamond grains and then polished with 2 μm-diamond particle slurry. Fig. 2 illustrates the geometry of a sample with cracks introduced by Vickers indentations. Three Vickers indentations were conducted at 49 N for 10 s in air on each sample to introduce pre-cracks at the center of the sample tension surface. Fig. 3 shows a cross-sectional view of a fractured Vickers indentation. The white arrow and dashed line indicate the Vickers indentation and front of the semi-elliptical crack introduced by the Vickers indentation, respectively. The crack depth was approximately 200 μm. As-cracked samples were heat-treated at temperatures ranging from 600 to 1200 °C for 1 and 6 h in air at a 400 K/h heating rate. Heat-treatment temperature was monitored using an R-type thermocouple located near the sample. Surface crack disappearance was evaluated fraction of surface crack length remaining heat treatment, ΔC, as follows:

$$\Delta C = \frac{1}{12}\left\{\left(1-\frac{C_1'}{C_1}\right)+\left(1-\frac{C_2'}{C_2}\right)+\cdots+\left(1-\frac{C_{12}'}{C_{12}}\right)\right\}\times 100 \quad (1)$$

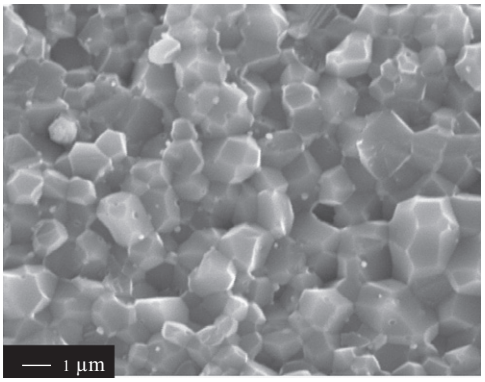

Fig. 1. SEM image of fractured surface of as-sintered sample.

where C_1, C_2, … C_{12} are the surface crack lengths of the 3 indentations before heat-treatment and C'_1, C'_2, … C'_{12} are the values after heat treatment. Fig. 4 shows schematic illustrations the method used to measure surface crack length.

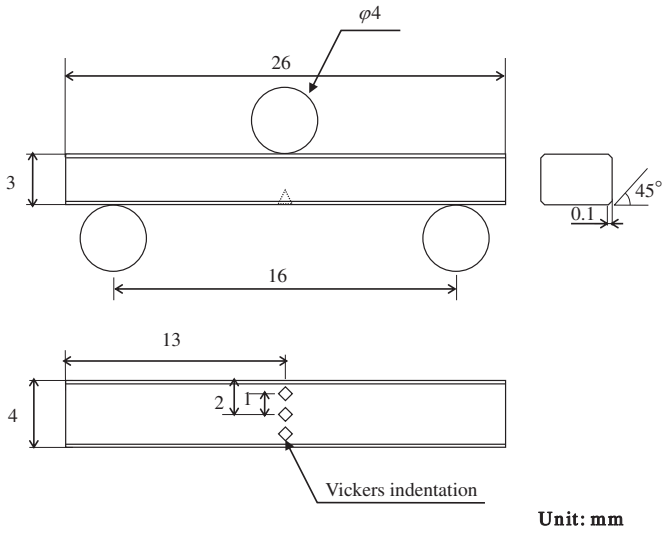

Fig. 2. Geometry of cracks introduced by Vickers indentations and the sample during three-point bending test.

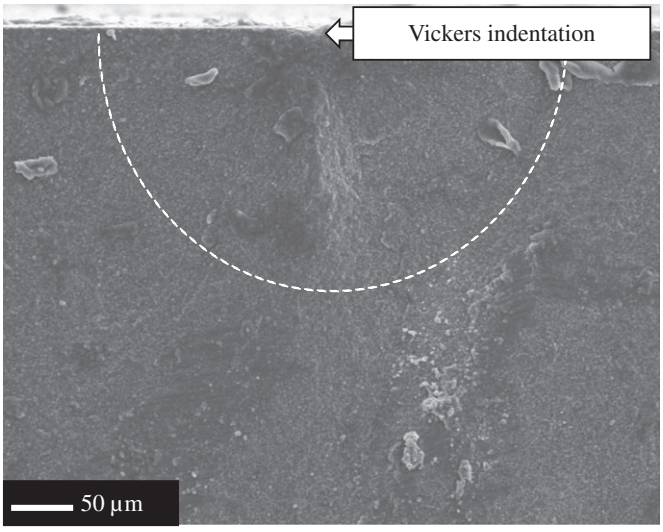

Fig. 3. Cross-sectional SEM image of fractured surface of as-cracked sample after bending test.

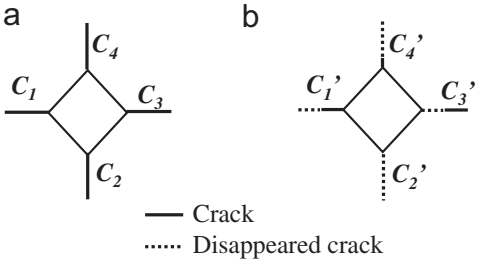

Fig. 4. Schematic illustrations of crack length measurement (a) before and (b) after heat treatment.

Each surface crack length was measured before and after heat-treatment using SEM.

Three-point bending tests (16-mm span length) were carried out with a cross-head speed of 0.5 mm/min at room temperature. Bending strength values were averaged by measuring 5 test pieces. Phase identification and microstructure of sample surfaces were conducted for bending tested specimens using XRD and SEM, respectively.

3. Experimental results

Fig. 5 shows SEM images of sample surfaces before and after heat-treatment at 600 to 1200 °C in air. Dashed lines outline the edges of the Vickers indentation. Well-propagated cracks on the sample surface from each corner of the imaged Vickers indentations can be observed in Fig. 5(a). Surface crack length and width near the vertex of the Vickers indentation were determined as approximately 60 and 1 μm, respectively. After heat-treatment at 600 °C for 1 h, white contrast particles were observed on the sample surface and cracks had partially disappeared, as shown in Fig. 5(b). With increasing temperature to 1000 °C, oxidation product developed on grain boundaries of the Al_2O_3 matrix, as shown in Fig. 5(c). Surface crack disappearance was initially recognized at the end of each surface crack and then the disappeared area extended to the corner of the Vickers indentation. As-shown in Fig. 5(d), heat-treated at 1200 °C for 1 h in air, the network-like oxidation products developed on and mostly covered the sample surface instead of particle-like products. After heat-treatment at 1200 °C for 6 h in air, surface crack disappearance was completed, as shown in Fig. 5(e).

XRD patterns of the surface of the samples are shown in Fig. 6. Although only Ni and α-Al_2O_3 peaks were identified for the as-sintered sample before heat-treatment, peaks attributed to $NiAl_2O_4$ appeared after heat-treatment in air. The intensity of these $NiAl_2O_4$ peaks became stronger with higher heat-treatment temperature and longer duration.

Fig. 7 shows bending strength and fraction of crack disappearance for samples heat-treated at 600 to 1200 °C for 1 h in air. Bending strength of the as-sintered samples was 490 ± 58 MPa. As-cracked sample bending strengths declined to 180 ± 15 MPa: this value was unchanged after heat-treatment at 600 °C for 1 h in air and increased slightly at 800 °C, while the fraction of surface crack disappearance remained ranging from 10 to 30%. Bending strength of samples heat-treated at 1000 °C for 1 h reached 550 ± 190 MPa, comparable with as-sintered ones. The fraction of surface crack disappearance was approximately 10% when samples were heat-treated at 1000 °C for 1 h in air. This increased up to 60% at 1200 °C for 1 h in air and the bending strength remained comparable with that of as-sintered samples. Fig. 8 shows bending strength of samples heat-treated in air at 1200 °C as function of heat-treatment time. Surface crack disappearance increased to 100%, that is, complete crack disappearance, whereas bending strength remained at approximately 550 MPa.

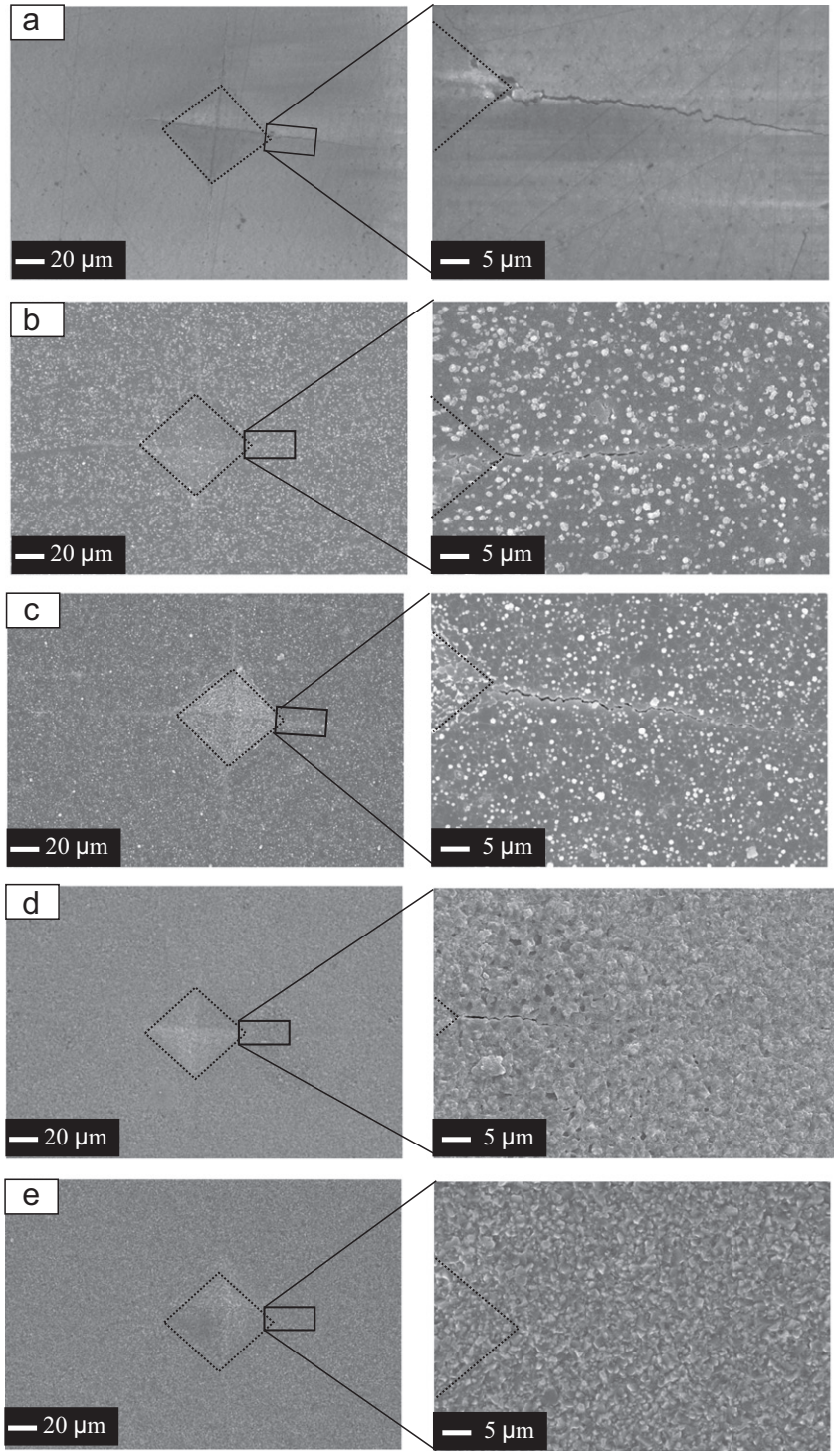

Fig. 5. SEM images showing surface views of (a) as-cracked sample and samples heat-treated at (b) 600 °C for 1 h, (c) 1000 °C for 1 h, (d) 1200 °C for 1 h and (e) 1200 °C for 6 h in air.

Fig. 9 shows SEM images of sample surfaces after bending tests. Dashed lines outline the edges of the Vickers indentation. As-cracked samples fractured along the Vickers indentations as shown in Fig. 9(a). The samples heat-treated at 1000 °C for 1 h in air were fractured both along the Vickers indentation and at a different position, as shown in Fig. 9(b). Samples heat-treated at 1200 °C for 6 h in air did not break along the Vickers indentations as shown in Fig. 9(c).

4. Discussion

As shown in Fig. 6, $NiAl_2O_4$ peaks intensities measured for the surface of sample oxidized in air increased with heat-treatment temperature and time. $NiAl_2O_4$ was the only new phase formed after heat-treatment. According to the ternary phase diagram of the Ni-Al-O system [25], NiO does not coexist with Al_2O_3. Nanko et al. [26] reported the high-

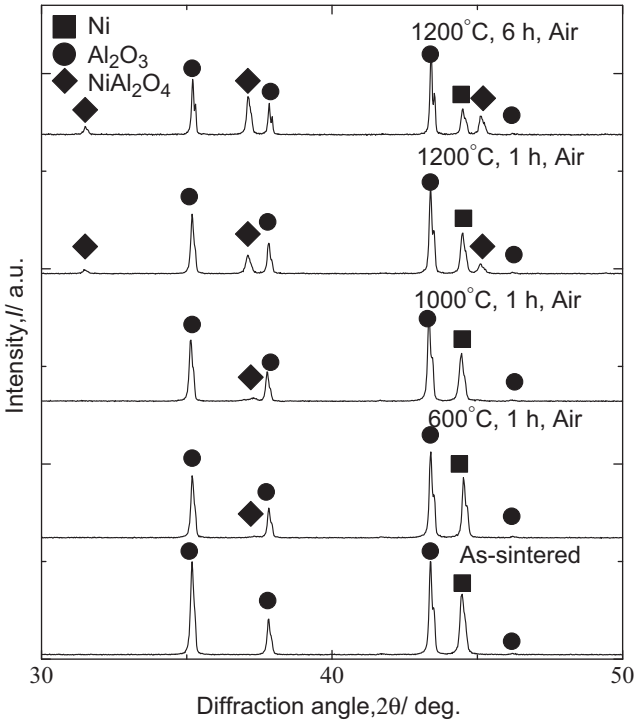

Fig. 6. XRD patterns for surfaces of heat-treated samples.

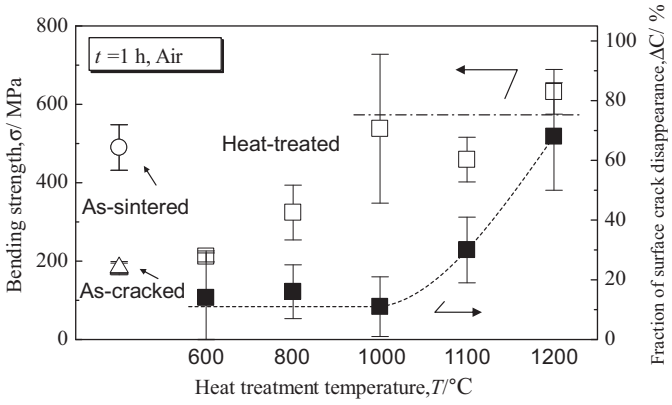

Fig. 7. Relationship between fraction of surface crack disappearance and bending strength for nano-Ni/Al_2O_3 heat-treated for 1 h in air as function of heat-treatment temperature.

temperature oxidation behavior of nano-Ni/Al_2O_3. In that study, a thin $NiAl_2O_4$ layer, 2–5 μm thickness, was observed on the surface of samples oxidized at 1300 °C for 1 d in air.

Bending strength was recovered due to the formation of oxidation product during heat-treatment in air. Brittle materials, such as ceramics, fracture from the largest defect causing the largest stress concentration. As-cracked samples were broken along surface cracks introduced by the Vickers indentations as shown in Fig. 9(a). Samples with cracks that had disappeared completely fractured at different positions to the indentation, as shown in Fig. 9(c), indicating that mechanical strength at the cracked region was repaired to the same level of the region without cracks. Yao et al. [27] revealed the crack-healing behavior of SiC/Si_3N_4 via heat-treatment at 1200 to 1400 °C for 1 h in air. Bending strength

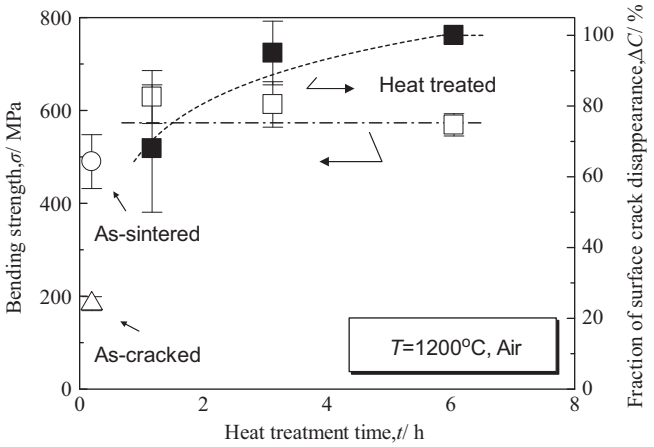

Fig. 8. Bending strength of samples heat-treated at 1200 °C in air as function of heat-treatment time.

was recovered due to formation of SiO_2 on the sample surface, and as a result, samples were broken in three-point bending tests at positions different to cracks introduced by the Vickers indentation.

Because brittle materials, such as alumina, typically break at the largest defect, recovery of mechanical strength can occur when remaining cracks are smaller than intrinsic defects. As shown in Fig. 7, when the fraction of surface crack disappearance was approximately 10% after heat-treatment at 1000 °C, bending strength increased to the level observed for as-sintered samples. After the fraction of surface crack disappearance reached 60% at 1200 °C for 1 h in air, the bending strength continued to be approximately 550 MPa. As shown in Fig. 8, this bending strength is comparable with that observed after complete surface crack disappearance (100%). To confirm the size of remaining cracks, Fig. 10 shows cross-sectional views of an as-cracked sample and a sample heat-treated at 1000 °C for 1 h in air ($\Delta C = 10\%$) prepared using cross-section polisher before bending tests. Straight (A) and divided cracks (B) are shown in Fig. 10(a). Crack (A) and crack (B) are regarded as the median crack and the lateral crack, respectively [28]. The median crack had 160 μm total length and extended to the sample interior surface, while the lateral crack was elongated parallel with the sample surface with an off-set of approximately 20 μm. The width of both cracks was approximately 1 μm. Fig. 10(b) displays cross-sectional SEM images for samples oxidized at 1000 °C for 1 h in air. Free space in the cracks was filled by $NiAl_2O_4$, the oxidation product of nano-Ni/Al_2O_3. Surface cracks measuring a few microns still remained at the sample surface. Micro-pores, less than 1 μm in diameter, were also observed in the $NiAl_2O_4$ that filled the cracks. Sakai mentioned that bending strength of ceramic materials is inversely proportional to grain size because of weakly-bonded grain boundaries [29]. The smallest intrinsic defect size required for sample fracture is as large as the grain size, thus micro-pores and remaining surface cracks may be small enough to ignore these failure criteria. Bending strength of sample heat-treated at 1000 °C for 1 h showed recovery of mechanical strength

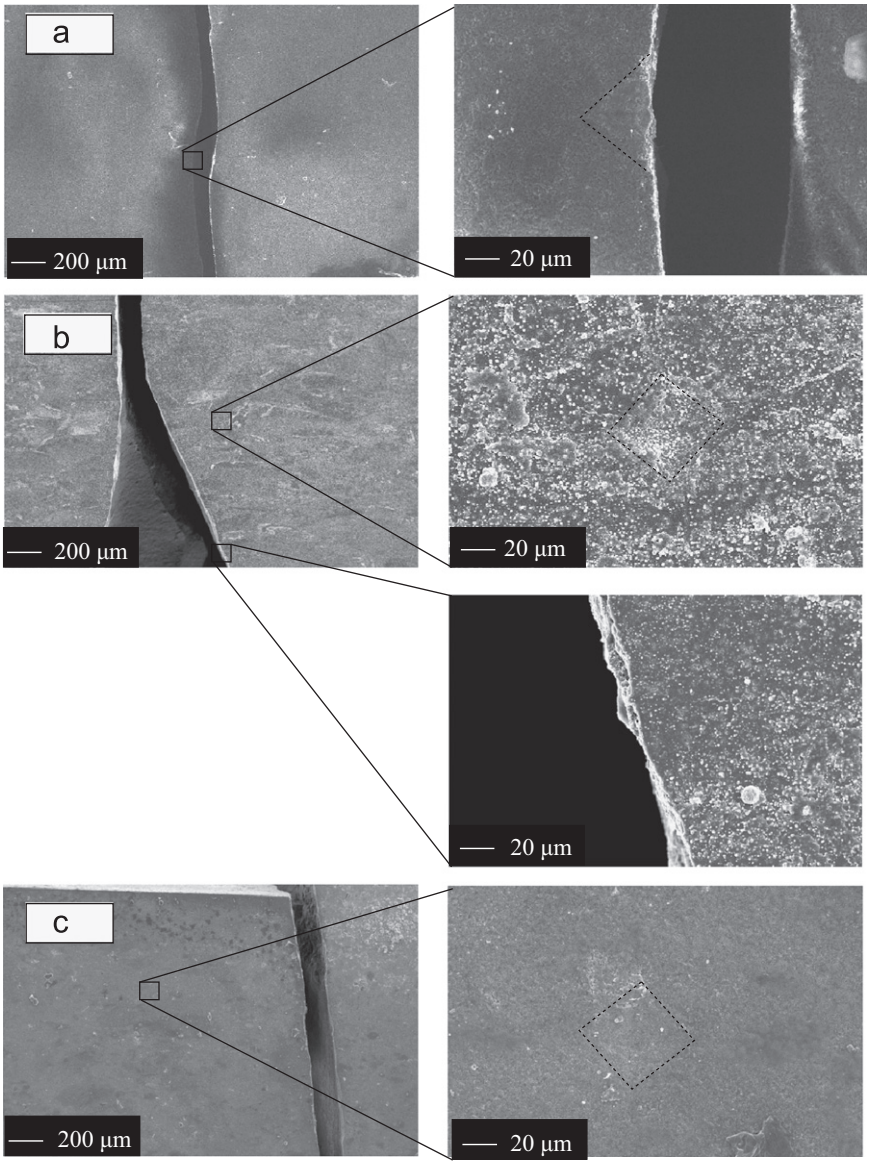

Fig. 9. SEM images of surface of bended samples (a) as-cracked, (b) heat-treated at 1000 °C for 1 h in air, and (c) heat-treated at 1200 °C for 6 h in air.

even though the fraction of surface crack disappearance was as low as 10%. The standard deviation of the bending strength of sample heat-treated at 1000 °C for 1 h was large compared with other heat-treatment conditions. This implies that this heat-treatment condition is at a transition point where recovery of mechanical strength begins. Crack depth introduced by Vickers indentation had small range in this experiment, and there were surface cracks that disappeared both enough and not enough to recover bending strength. The fact that the sample shown in Fig. 9(b) was fractured both along the Vickers indentation and at a different position also supports the large standard deviation measured for the heat-treatment of 1000 °C for 1 h in air.

To reveal the criteria for recovery of mechanical strength, Fig. 11 shows relationship between sample bending strength as a function of fraction of surface crack disappearance. The values of bending strength were mostly scattered in the low surface crack disappearance region from 5 to 55%, as shown in the gray area in Fig. 11. This gray area indicates the transition of the failure criteria from the introduced cracks to the intrinsic defects. Bending strength remained slightly higher in heat-treated samples compared with as-sintered ones when the fraction of surface crack disappearance is increased to approximately 50%. The criteria of failure shifted to other defects such as intrinsic defects. Bending strength was constant at approximately 604 MPa when fraction of surface crack disappearance was over 55%.

A speculative mechanism of crack disappearance in nano-Ni/Al_2O_3 systems was proposed as shown in Fig. 12. When nano-Ni/Al_2O_3 is heat-treated in an atmosphere in which Ni is oxidized, granular-shaped $NiAl_2O_4$ is formed on the sample surface at the early stage of heat treatment, such as that shown in Fig. 5(a) and (b). This granular $NiAl_2O_4$ is formed by nano-Ni particles on the surface reacting with oxygen and surrounding Al_2O_3. Recovery of mechanical strength in this system occurred when crack-tips are covered

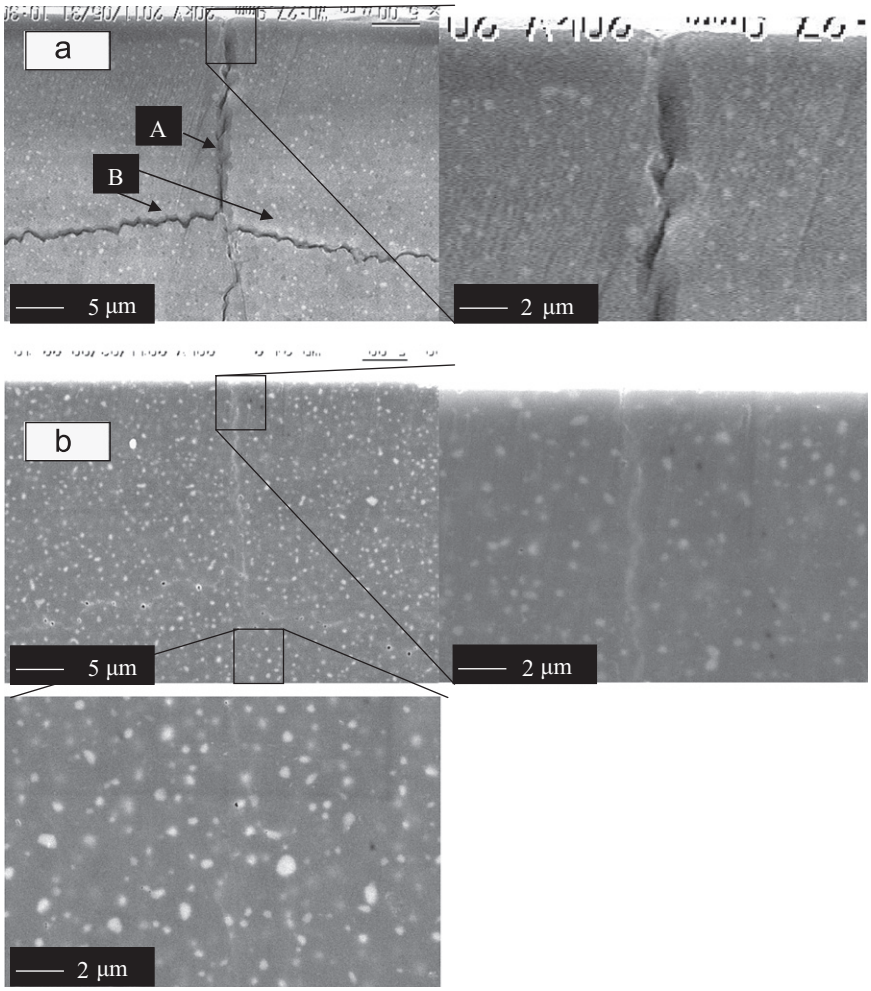

Fig. 10. Cross-sectional views of nano-Ni/Al_2O_3 (a) as-cracked and (b) heat-treated at 1000 °C for 1 h in air.

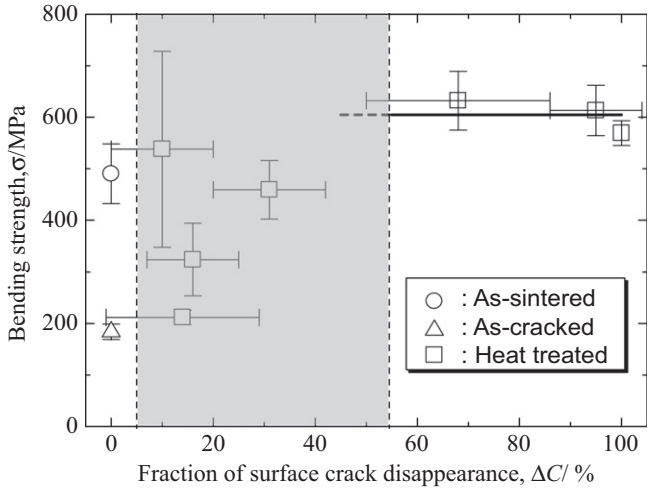

Fig. 11. Bending strength of samples as function of fraction of surface crack disappearance for various heat treatment conditions.

by $NiAl_2O_4$, thus granular $NiAl_2O_4$ does not influence to the recovery of mechanical strength, as shown in Fig. 12(b). Network-like $NiAl_2O_4$ was also observed in Fig. 5(d). The size of the network was approximately 1 μm, which is comparable with Al_2O_3 grain size. It is obvious that the network-like $NiAl_2O_4$ formed on grain boundaries on the surface of Al_2O_3 matrix. Because a supply of Ni ions is required to form $NiAl_2O_4$ along these grain boundaries, outward diffusion of cations occurred during heat treatment. According to Nanko [30], while the dominant oxidation process in nano-Ni/Al_2O_3 system is inward diffusion of oxide ions, cation diffusion also contributed. Both diffusions of ions occurred simultaneously as shown in Fig. 12(c). Since the crack-tip is covered by even partial crack disappearance, recovery of mechanical strength occurs relaxation of stress concentration at the crack-tip. Although cracks remained after heat-treatment at 1000 °C for 1 h in air, the inside of the crack was likely partially filled with oxidation product, which recovered its bending strength. Finally, crack disappearance is completed by formation of $NiAl_2O_4$ as shown in Fig. 12(d).

5. Conclusions

In this study, recovery of mechanical strength as a function of heat-treatment temperature and time was investigated for nano-Ni/Al_2O_3 via fraction of surface crack disappearance. Bending strengths of as-sintered and as-cracked samples were

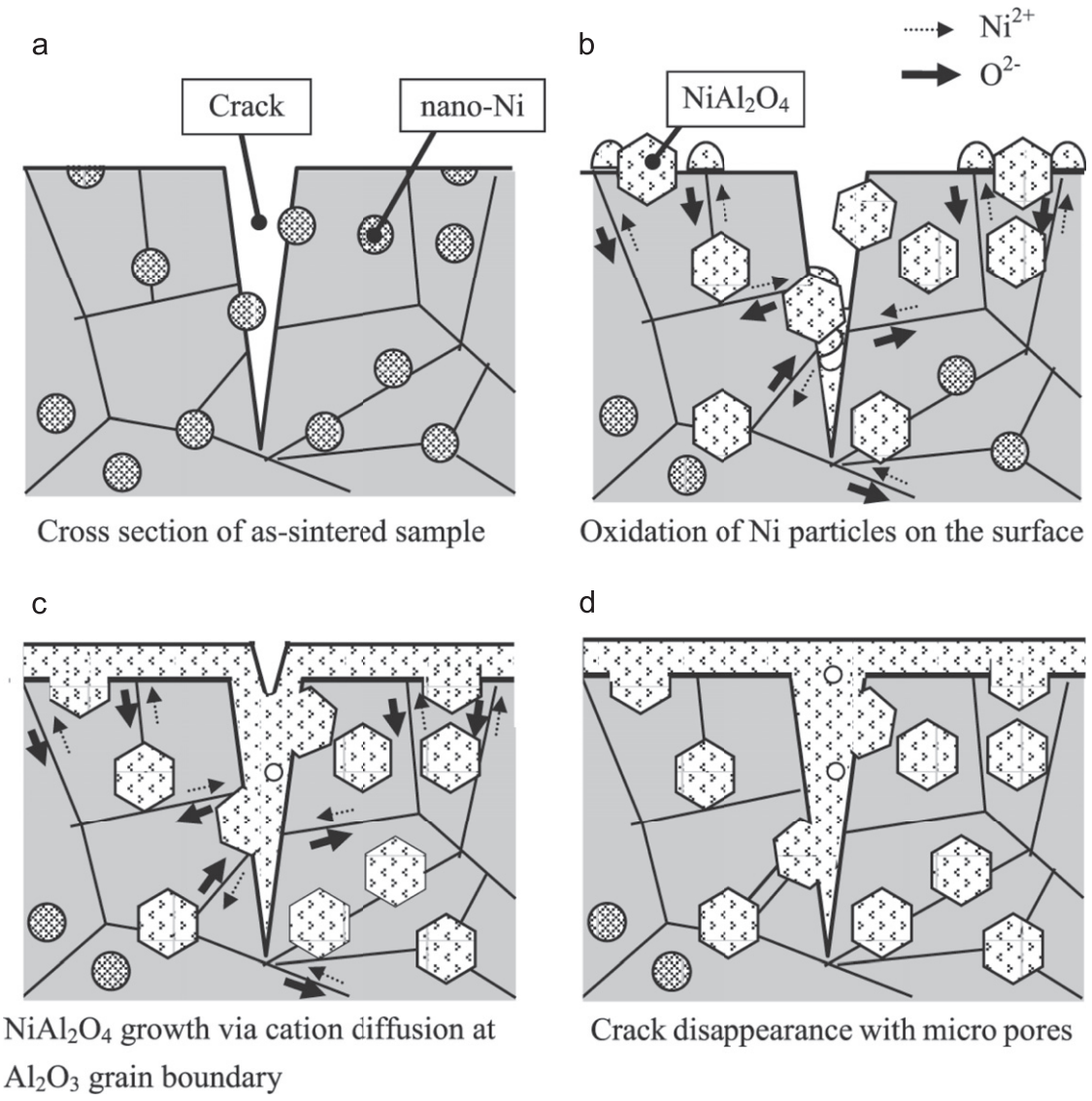

Fig. 12. Speculative illustrations of kinetic model for oxidation during crack-healing.

approximately 490 ± 58 and 180 ± 15 MPa, respectively. Bending strength was decreased by introduction of surface cracks (approximately 200 μm in depth) and began to recover to 550 ± 190 MPa by heat-treatment at 1000 °C for 1 h in air, which was comparable with that of as-sintered samples. The fraction of surface crack disappearance was approximately 10%. The bending strengths of samples heat-treated at higher temperatures or for a longer time were also comparable with those of the as-sintered ones.

Because bending strength of as-cracked samples was recovered by only partial crack disappearance on the sample surface, the observed recovery of mechanical strength was caused by a reduction of stress concentration at crack-tips covered by the formation of $NiAl_2O_4$. The relationship between recovery of mechanical strength and fraction of surface crack disappearance showed that recovery of mechanical strength for nano-Ni/Al_2O_3 can be expected to be achieved when the fraction of surface crack disappearance is over 50%, and depends on crack condition such as crack depth and width. Network-like $NiAl_2O_4$ was observed on the surface of samples oxidized at 1000 °C for 1 h in air, indicating that $NiAl_2O_4$ formed mostly by diffusion of Ni^{2-} along grain boundaries of the Al_2O_3 matrix.

Acknowledgment

I have had the support and encouragement of Prof. S. Kamado and Dr. T. Honma from the Nagaoka University of Technology for operation of the cross-section polisher.

References

[1] H. Awaji, Strength of Ceramic Materials, First Edition, Corona Publication, Tokyo, 2001 in Japanese.
[2] M.C. Chu, S. Sato, Y. Kobayashi, K. Ando, Damage healing and strengthening behaviour in intelligent mullite/SiC ceramics, Fatigue and Fracture of Engineering. Materials and Structures 18 (1995) 1019–1029.

[3] S.K. Lee, M. Ono, W. Nakao, K. Takahashi, K. Ando, Crack-healing behaviour of mullite/SiC/Y_2O_3 composites and its application to the structural integrity of machined components, Journal of the European Ceramic Society 25 (2005) 3495–3502.
[4] K.W. Nam, J.S. Kim, Critical crack size of healing possibility of SiC ceramics, Materials Science and Engineering A 527 (2010) 3236–3239.
[5] I.A. Chou, H.M. Chan, M.P. Harmer, Effect of annealing environment on the crack healing and mechanical behavior of silicon carbide-reinforced alumina nanocomposites, Journal of the American Ceramic Society 81 (1998) 1203–1208.
[6] J. Lu, Z.X. Zheng, Y.C. Wu, Z.H. Jin, High temperature crack healing of Al_2O_3 -matrix composites, Journal of Advanced Materials 37 (2005) 63–69.
[7] T. Arima, Y. Hirata, N. Matsunaga, M. Shibuya, Influence of crack healing on mechanical properties of SiC fabric/ SiC–Al_2O_3 matrix laminates, Key Engineering Materials 352 (2007) 49–52.
[8] H. Zhai, J. Li, X. Huang, Bending strength recovery and crack healing behavior of Al_2O_3/SiC nanocomposites at different annealing temperatures, Key Engineering Materials 224–226 (2002) 325–330.
[9] K. Houjou, K. Ando, S.P. Liu, S. Sato, Crack-healing oxidation behavior of silicon nitride ceramics, Journal of the European Ceramics Society 24 (2004) 2329–2338.
[10] K. Takahashi, M. Yokouchi, S.K. Lee, K. Ando, Crack-healing behavior of Al_2O_3 toughened by SiC whiskers, Journal of the American Ceramic Society 86 (2003) 2143–2147.
[11] T. Osada, W. Nakao, K. Takahashi, K. Ando, S. Saito, Strength recovery behavior of machined Al_2O_3/SiC nano-composite ceramics by crack-healing, Journal of the American Ceramic Society 27 (2007) 3261–3267.
[12] W. Nakao, K. Takahashi, K. Ando, Self-healing of surface crack in structural ceramics, in: S.K. Ghosh (Ed.), Self-healing Materials, Fundamentals, Design Strategies, and Applications, WILEY-VCH, Weinheim, 2009, pp. 183–217.
[13] K.W. Nam, Crack-healing behavior and bending strength of Al_2O_3/SiC composite ceramics according to the amount of added Y_2O_3, Journal of Ceramic Processing Research 11 (2010) 471–474.
[14] O. Abe, Y. Ohwa, Y. Kuranobu, Possibility of enhanced strength and self-recovery of surface damages of ceramics composites under oxidative conditions, Journal of the European Ceramic Society 26 (2005) 689–695.
[15] J. Lu, Z.X. Zheng, H.F. Ding, Z.H. Jin, Preliminary study of the crack healing and strength recovery of Al_2O_3-matrix composites, Fatigue and Fracture of Engineering. Materials and Structures 27 (2004) 89–97.
[16] A.L. Salas-Villasenor, J. Lemus-Ruiz, M. Nanko, D. Maruoka, Crack disappearance by high-temperature oxidation of alumina toughened by Ni nano-particles, Advanced Materials Research 68 (2009) 34–43.
[17] D. Maruoka, M. Nanko, Crack-healing effectiveness of nano Ni+SiC Co-dispersed alumina hybrid materials, Advanced Materials Research 89–91 (2010) 365–370.
[18] K. Niihara, New design concept of structural ceramics: Ceramic nanocomposites, Journal of the Ceramic Society of Japan 99 (2000) 974–982.
[19] M. Nawa, T. Sekino, K. Niihara, The sintering mechanism of Al_2O_3/SiC nanocomposite, Journal of the Japan Society of Powder and Powder Metallurgy 39 (1992) 484–487.
[20] T. Matsunaga, U. Leela-Adisorn, Y. Kobayashi, S.M. Choi, H. Awaji, Fabrication of alumina-based toughened nanocomposites, Journal of the Ceramic Society of Japan 113 (2005) 123–125.
[21] B.S. Kim, T. Sekino, T. Nakayama, M. Wada, J.S. Lee, K. Niihara, Pulse electric current sintering of alumina/nickel nanocomposites, Materials Research Innovations 7 (2003) 57–61.
[22] G. Li, X. Huang, J. Guo, Fabrication and mechanical properties of Al_2O_3–Ni composite from two different powder mixtures, Materials Science and Engineering A 352 (2003) 23–28.
[23] M. Liberthal, W.D. Kaplan, Processing and properties of Al_2O_3 nanocomposites reinforced with sub-micron Ni and $NiAl_2O_4$, Materials Science and Engineering A 302 (2001) 83–91.
[24] T. Sekino, T. Nakajima, T. Ueda, K. Niihara, Reduction and sintering of a nickel-dispersed-alumina composite and its properties, Journal of the American Ceramic Society 80 (1997) 1139–1148.
[25] K.P. Trumble, M. Ruhle, The thermodynamics of spinel interphase formation at diffusion-bonded Ni/Al_2O_3 interfaces, Acta Metallurgica et Materialia 39 (1991) 1915–1924.
[26] M. Nanko, M. Mizumo, M. Watanabe, K. Matsumaru, K. Ishizaki, High-temperature oxidation of nano-Ni dispersed Al_2O_3 composites in air, Advances in Technology of Materials and Materials Processing Journal 6 (2004) 240–243.
[27] F. Yao, K. Ando, M.C. Chu, S. Sato, Crack-healing behavior, high temperature and fatigue strength of SiC-reinforced silicon nitride composite, Journal of Materials Science Letters 19 (2000) 1081–1083.
[28] K. Niihara, R. Morena, D.P.H. Hasselman, Evaluation of K_{1C} of brittle solids by the indentation method with low crack-to-indent ratios, Journal of Materials Science Letters 1 (1982)13-16 1 (1982).
[29] M. Sakai, The quest of fracture mechanism of ceramic materials, Bulletin of Ceramic Society of Japan 27 (1992) 281–287 in Japanese.
[30] M. Nanko, K. Matsumaru, K. Ishizaki, Role of cation diffusion on high temperature oxidation of metal dispersed ceramic matrix composites, Advances in Technology of Materials and Materials Processing Journal 7 (2005) 5–8.